

## Naphthalene Diimide Based Materials with Adjustable Redox Potentials: Evaluation for Organic Lithium-Ion Batteries

Geeta S. Vadehra, Ryan P Maloney, Miguel A. Garcia-Garibay, and Bruce Dunn

*Chem. Mater.*, **Just Accepted Manuscript** • DOI: 10.1021/cm503800r • Publication Date (Web): 01 Dec 2014

Downloaded from <http://pubs.acs.org> on December 5, 2014

### Just Accepted

“Just Accepted” manuscripts have been peer-reviewed and accepted for publication. They are posted online prior to technical editing, formatting for publication and author proofing. The American Chemical Society provides “Just Accepted” as a free service to the research community to expedite the dissemination of scientific material as soon as possible after acceptance. “Just Accepted” manuscripts appear in full in PDF format accompanied by an HTML abstract. “Just Accepted” manuscripts have been fully peer reviewed, but should not be considered the official version of record. They are accessible to all readers and citable by the Digital Object Identifier (DOI®). “Just Accepted” is an optional service offered to authors. Therefore, the “Just Accepted” Web site may not include all articles that will be published in the journal. After a manuscript is technically edited and formatted, it will be removed from the “Just Accepted” Web site and published as an ASAP article. Note that technical editing may introduce minor changes to the manuscript text and/or graphics which could affect content, and all legal disclaimers and ethical guidelines that apply to the journal pertain. ACS cannot be held responsible for errors or consequences arising from the use of information contained in these “Just Accepted” manuscripts.

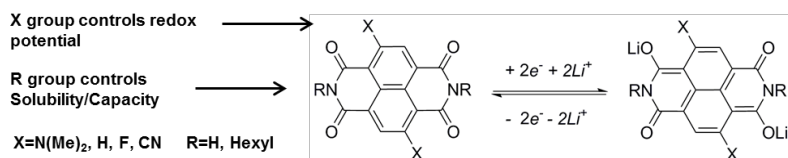


# Naphthalene Diimide Based Materials with Adjustable Redox Potentials: Evaluation for Organic Lithium-Ion Batteries

Geeta S. Vadehra, Ryan P. Maloney, Miguel A. Garcia-Garibay\*, Bruce Dunn\*

Department of Chemistry and Biochemistry, University of California, Los Angeles, California 90095, Department of Materials Science and Engineering, University of California, Los Angeles, California 90095.

**ABSTRACT:** The promising crystallinity and tunable redox capabilities of naphthalene diimides make them attractive candidates as electroactive materials for organic-based lithium-ion batteries. In this study, a family of naphthalene diimide derivatives was synthesized and their redox properties explored with the intent of unveiling structures with reduction potentials that are higher than those encountered in previous organic redox processes. Changes in the electronic characteristics of the aryl substituents resulted in materials with discharge potentials that vary from 2.3 to 2.9 V vs. Li/Li<sup>+</sup>, with discharge capacities as high as 121 mAh/g.



## INTRODUCTION

Lithium ion batteries have achieved enormous success in the area of energy storage in small electronics due to their impressive energy densities and cyclability.<sup>1,2</sup> These batteries are based on the use of Li intercalation compounds. Li ions are transported between two host structures, a graphite negative electrode that is electrochemically connected by a non-aqueous electrolyte to the positive electrode, commonly a transition metal oxide compound. With an output voltage of ~4 V this process works relatively well, however, the required metal oxides (LiCoO<sub>2</sub>, LiNiO<sub>2</sub>, LiMn<sub>2</sub>O<sub>4</sub>) have some drawbacks: they are relatively scarce, heavy, toxic and their production requires expensive high temperature processing.<sup>3</sup> In recent years, there has been growing interest in creating electroactive organic electrode materials that use natural organic sources as precursors and generally lead to environmentally benign processing.<sup>4</sup>

Many of these concerns can be addressed by taking advantage of organic electrodes based on bulk crystals of suitable redox active compounds. First explored in the early 1970s,<sup>5</sup> organic redox-active compounds tend to be less expensive, less toxic and potentially much lighter than their inorganic counterparts. Their performance, however, has been limited by their inability to reach high redox potentials, and by their tendency to dissolve in non-aqueous electrolytes, which limits their use to a few charge-discharge cycles. Nonetheless, as the limits of inorganic insertion metal oxides are being reached, organic redox materials are being revisited.<sup>6</sup> Recent work

has focused on increasing cycling capabilities by decreasing their solubility<sup>6-10</sup> with the use of rigid aromatics<sup>9,10,11</sup> or insoluble salts<sup>6,9</sup>. However, their lithium-insertion potentials are still too low to compete with the nearly 4 V vs Li/Li<sup>+</sup> observed with other transition metal oxides. As illustrated in Table 1, research in organic electrodes thus far has incorporated three main categories of organic redox-active functionalities:<sup>7,12</sup> nitroxyl radicals, disulfides, and conjugated dicarbonyls.

Nitroxyl radicals<sup>13</sup> can be oxidized with potentials of ca. 3.5-3.6 V vs. Li/Li<sup>+</sup>. The cationic charged state of this mechanism designates it as a “p-type” redox mechanism. This narrow range is determined by its relatively isolated two-atom (N-O) redox system. Furthermore, having a one-electron redox mechanism results in a more limited energy storage capacity in comparison to the two-electron processes displayed by disulfides<sup>14,15</sup> and conjugated dicarbonyls.<sup>6,8,9,16</sup> In addition, considering that nitroxyls are oxidized in the charging process, their function depends on the insertion of charge-compensating stable anions. The large anions such as PF<sub>6</sub><sup>-</sup> that are common in Li-ion electrolytes cannot be inserted readily into the corresponding material.

The two-electron reduction of disulfides into the corresponding lithium thiolate species, illustrated with derivative **2**, is also not ideal. Disulfides display a relatively low potential, typically ranging from 1.8-2.3 V vs. Li/Li<sup>+</sup>,<sup>17</sup> and have a redox mechanism that seems not to lend itself to large electronic variations due to the isolated nature of

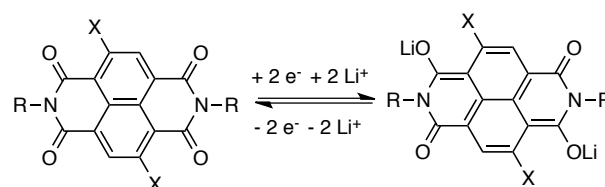
**Table 1.** Summary of processes typical to each category: disulfide bond, nitroxide radicals and conjugated carbonyls.

Redox Structure	Category	Discharge Potential (V vs Li/Li <sup>+</sup> )	Redox Type	Theoretical Capacity (mAh/g)	Reference
	Nitroxyl Radical	3.5	p-type	111	13
	Disulfide	1.8	n-type	282	15
	Dicarbonyl	1.7	n-type	235	9
	Dicarbonyl	0.8	n-type	301	18
	Dicarbonyl	2.3	n-type	257	17

this particular functional group. In contrast, the reduction of conjugated carbonyls into the corresponding dialkoxides seem to have a larger range of molecular design and electronic tunability.<sup>8,16-18</sup> For example, compounds **3**, **4** and **5** in Table 1 display two-electron redox processes with potentials that cover a range from 0.8 V for dicarboxylate **4** and up to 2.3 V for anthraquinone **5** with a mid-point value of 1.7 V for pyromellitic diimide **3**. These variations demonstrate the relatively large range available for this redox process and the potential for fine-tuning and optimizing the observed potential.

In this paper, we use a model system, naphthalene diimide (NDI; see Figure 1), to explore the possibility of extending the range of physical properties and redox parameters. We expect that an extended aromatic core as compared to that of pyromellitic diimide **3** should serve the dual purpose of decreasing the solubility of the crystalline material while providing opportunities to modify the LUMO levels of the parent hydrocarbon structure **6** (Figure 1, X=H) with the help of synthetically accessible substituents. Knowing that a highly desirable low solubility translates into very challenging sample tractability during synthesis and analysis, we decided to analyze two sets of structures with (R=C<sub>6</sub>H<sub>13</sub>) and without (R=H) an N-hexyl substituent. In this article we report the synthesis and electrochemical evaluation of compounds with a hydrocarbon aromatic core (X=H), as

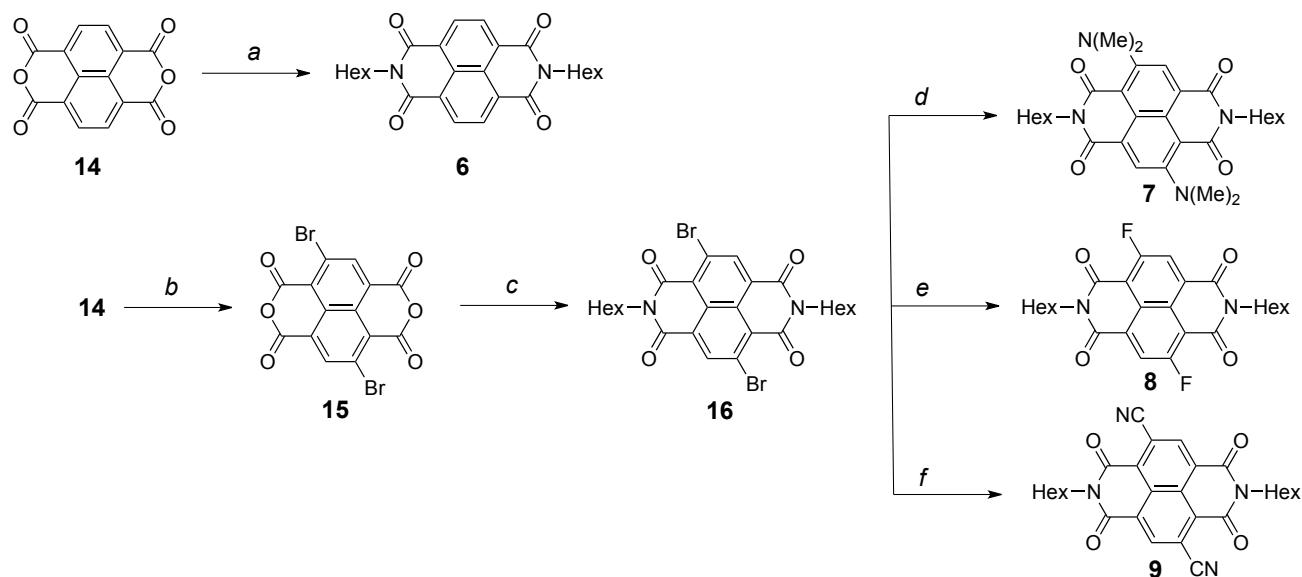
well compounds with electron donating X=NMe<sub>2</sub> (**7** and **11**), and electron withdrawing X=F (**8** and **12**) and X=CN (**9** and **13**) substituents (Figure 1).<sup>19</sup> The decreased electron density of the NDI core was expected to increase the potential of **9** as compared to that of **6** without drastically compromising its capacity.



Compound	X	R
<b>6</b>	H	Hexyl
<b>7</b>	NMe <sub>2</sub>	Hexyl
<b>8</b>	F	Hexyl
<b>9</b>	CN	Hexyl
<b>10</b>	H	H
<b>11</b>	NMe <sub>2</sub>	H
<b>12</b>	F	H
<b>13</b>	CN	H

**Figure 1.** Structure and redox process of naphthalene diimides (NDIs) with different aromatic (X) and imide (R) substituents. Although there is a potential four electron mechanism resulting in the lithiation of the remaining carbonyls, attempts to reach sufficiently low potentials to access this state resulted in irreversible decomposition.<sup>19</sup>

Scheme 1



(a) Hexylamine, pyridine, 120°C, 83%; (b) Dibromoisocyanuric acid, sulfuric acid, 130°C; (c) Hexylamine, glacial acetic acid, 100°C, 40% over two steps; (d) Dimethylamine, THF, 80°C, 93%; (e) KF, 18-crown-6, 3 Å molecular sieves, sulfolane, 165°C, 53%; (f) CuCN, NMP, 100°C, 87%.

## EXPERIMENTAL

**Materials Synthesis.** All the naphthalene diimides studied in this work were synthesized by the procedures indicated in Schemes 1 and 2. Their characterization and purity were determined by standard spectroscopic techniques (please see SI).

**Electrode preparation.** Electrodes were prepared by drop casting a slurry of the electroactive material, acetylene black (Alfa Aesar #39724) conductive additive, and polyvinylidene fluoride (PVDF) binder (Kynar PVDF) onto pre-cut current collectors, which were allowed to dry under ambient conditions. The slurries had a nominal composition of 45:50:5 electroactive material:carbon:PVDF, with the PVDF dissolved in N-methyl pyrrolidone (NMP) prior to addition to the slurry. Enough NMP (Sigma Aldrich #443778) was added to form a paint-like consistency; nominally 800  $\mu\text{L}$  NMP per 100mg of dry material (inclusive of the NMP used to dissolve the PVDF). A volume of 30  $\mu\text{L}$  of slurry was pipetted onto each 3/8" diameter carbon-coated aluminum current collector (Exopac Z-Flo 2650), resulting in an average areal loading of 6 mg  $\text{cm}^{-2}$ .

**Electrochemical Characterization in Solution:** The compounds were cycled in 0.1 M tetrabutylammonium hexafluorophosphate in  $\text{CH}_2\text{Cl}_2$ . A platinum wire and platinum disk were used for working and counter electrodes, respectively, and the working potential was measured versus a Ag/AgCl reference electrode.<sup>20</sup>

**Electrochemical Characterization in the Solid State:** Electrodes were tested in a 2016 coin cell with 1M  $\text{LiClO}_4$  in 1:1 vol/vol ethylene carbonate : dimethyl carbonate (EC:DMC) electrolyte, using lithium metal as counter electrode and Celgard #3401 separator. Minimum electrolyte volume was used in order to moisten the separa-

tor. The cells were assembled in an Argon filled glove box containing less than 1 ppm water and oxygen. Electrochemical characterization was performed using a Biologic VMP-3 system. Each cell was characterized by cyclic voltammetry (CV) at multiple sweep rates and galvanostatic cycling at a C/5 rate based on the theoretical two-electron capacity of the electroactive material.

## RESULTS AND DISCUSSION

**LUMO Energies.** As a starting point for this study, and to guide our electrochemical measurements, we looked for qualitative insight into the effects of substituents on the aromatic core of the NDI units. Calculations were carried out using gas phase electronic structure calculations with the B<sub>3</sub>LYP/6-311+G(d,p) level of theory for both the N-hexyl and the N-H compounds in order to establish the LUMO values versus their neutral states, which are known to correlate directly to redox potentials.<sup>19</sup> As shown in Table 2, the LUMO levels of N-hexyl compounds 6-9 span an energy range of 1.5 eV from the more electron-rich dimethyl-amino substituted NDI 7, with a value of -3.0 eV, to the electron-poor cyano substituted NDI 9, which has a value of -4.5 eV. The unsubstituted core of compound 6 and the fluorine-substituted core of NDI 8 have similar values of -3.7 eV and -3.9 eV, respectively. The larger variation observed with respect to the parent compound in the case of 7 and 9 as compared to 8 confirm a greater effect for resonance effects relative to the inductive effects of the electronegative fluorine atom. Calculations also showed that removal of the N-hexyl groups in compounds 10-13 systematically shifts the corresponding energies by ca. -0.2 to -0.3 eV, with an increase in the range of values up to 1.6 eV between 11 (X=NMe<sub>2</sub>) and 13 (X=CN).

Table 2. Solid State Electrochemical Properties of Naphthalene Diimides 6-13.

NDI	X	R	MW	Theoretical Capacity (2e) [mA h g <sup>-1</sup> ]	Experimental Capacity at C/5 rate [mA h g <sup>-1</sup> ] <sup>a</sup>	Experimental Capacity at C/5 rate [# Li]	LUMO [eV] <sup>b</sup>	1 <sup>st</sup> Reducton Potential [V vs Li/Li <sup>+</sup> ] <sup>c</sup>
6	H	Hexyl	434.5	123	92	1.5	-3.7	2.5
7	NMe <sub>2</sub>	Hexyl	520.7	103	41	0.8	-3.0	2.3
8	F	Hexyl	470.5	114	45	0.8	-3.9	2.6
9	CN	Hexyl	484.5	111	100	1.8	-4.5	2.8
10	H	H	266.2	201	121	1.2	-4.0	2.55
11	NMe <sub>2</sub>	H	352.3	152	30	0.4	-3.2	2.4
13	CN	H	316.2	170	34	0.4	-4.8	2.9

<sup>a</sup> A C/5 rate is the value needed for the current to reach maximum theoretical capacity to be delivered in 5 h. <sup>b</sup> Gas phase values obtained with the B<sub>3</sub>LYP/6-311+G(d,p) level of theory. <sup>c</sup> Values obtained using solid state NDI electrodes during the galvanostatic cycling experiments.

*Aryl-Substituted N-Hexyl Naphthalene Diimides.* An experimental evaluation of the effect of aryl substituents on the reduction potential of the more soluble N-hexyl substituted NDIs 6-9 was carried out both in solution and in a coin cell format. The synthesis of these compounds was accomplished as illustrated in Scheme 1 starting from naphthalene tetracarboxylic dianhydride 14. Compound 6 was obtained in a single step in 83% yield by reaction of 14 with hexylamine. Compounds 7, 8 and 9 were obtained from the N-hexyl-dibromonaphthalenetetracarboxylic diimide 16, which was obtained from readily available dibromo naphthalenetetracarboxylic dianhydride 15.

Compound 7 was isolated as a dark blue solid in 93% yield via S<sub>N</sub>Ar reaction of NDI 16 with dimethyl amine. The fluorinated NDI 8 could be obtained via the hallex process<sup>21</sup> in 53% yields, and the cyano derivative 9 via copper-mediated coupling.<sup>22</sup> All compounds were obtained as solids and the purity was established by thin-layer chromatography and NMR spectroscopy. Cyclic voltammetric analysis of N-Hexyl NDIs 6-9 was carried out at ambient temperature at a 0.01 mM concentration of active material in 0.1 M tetrabutylammonium hexafluorophosphate in CH<sub>2</sub>Cl<sub>2</sub> (Figure 2). While the result obtained in dilute solution are not representative of the electrochemical behavior of the solid state material in a typical lithium-ion cell, they provide valuable information on the number of redox events and their reversibility or lack thereof. As shown in Figure 2 and in agreement with literature reports with other NDIs,<sup>21-23</sup> each compound exhibits two redox waves characteristic of the two-electron redox process indicated in Figure 1. The first redox wave results in a charge delocalized radical anion, and the second then results in the previously discussed dianion. It is important to point out that all the samples could be reversibly cycled. The effect of the substituent can be seen by the shift of the redox potentials in the figure from the electron donating N,N-dimethyl-aryl substituted NDI 7, shown at the bottom with the most negative potential vs Ag/AgCl, to the

most electron withdrawing cyano-aryl substituted NDI 9, with least negative potential at the

#### E(1/2) V vs Ag/AgCl (vs Li/Li+) in Dichloromethane

	X/X <sup>-</sup>	X <sup>-</sup> /X <sup>2-</sup>	LUMO (eV)
6	-0.64 (2.6)	-1.03 (2.21)	-3.7
7	-0.97 (2.27)	-1.23 (2.01)	-3.0
8	-0.55 (2.69)	-0.98 (2.26)	-3.9
9	-0.10 (3.14)	-0.64 (2.6)	-4.5

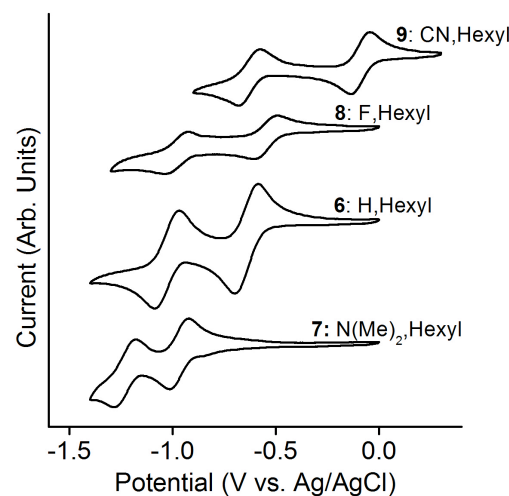


**Figure 2.** (a) Cyclic voltammograms of NDIs 6-9 measured vs Ag/AgCl in 0.1 M Bu<sub>4</sub>NPF<sub>6</sub> in CH<sub>2</sub>Cl<sub>2</sub> (Li/Li<sup>+</sup> is -3.237 vs Ag/AgCl).

top. It is clear from the figure and Table 2 that the effects of substituents are greatest on the first reduction potential as the difference between the first and second reduction wave decreases as the aromatic substituents change from electron withdrawing -CN (9) and -F (8), to the reference compound -H (6) to the electron rich -NMe<sub>2</sub> (7). In the case of NDI 9, the first reduction of the electron poor aromatic core occurs at a potential of -0.10 V vs Ag/AgCl and the second reduction wave occurs at a

more negative potential of  $-0.64$  V. By contrast, the comparatively electron-rich aromatic core of NDI **7** undergoes the first and second reduction waves much closer together, at values of  $-0.97$  V and  $-1.23$  V, with a difference between them that is about half as large as that of the two reduction peaks in **9**.

Having explored the effect of aryl substitution on the redox potential of NDIs **7-9** in solution, we next explored their effect on the potential and capacity in a coin cell format. The four N-Hexyl compounds were characterised both by cyclic voltammetry and galvanostatic cycling. As shown on the left column in Figure 3, the CV curves obtained with the solid electrodes when cycled between 1 and 4 V vs  $\text{Li/Li}^+$  revealed pronounced differences in shape as compared to those obtained in solution (Figure 2). Only NDI **6** exhibits two clear redox peaks (Figure 3a) while the others have a relatively large shift in the position of the peak and a significant broadening, suggesting kinetic limitations associated with electron and  $\text{Li}^+$  ion transport in the bulk solid material.

The galvanostatic cycling experiments measure the cell potential during the time that it takes to cycle between two potentials as a function of a constant pre-determined applied current. The current used in these experiments (generally known as the C-rate) was based on the theoretical capacity for a given sample being reached in 5 h; a value commonly referred to as a C/5 cycling rate (Table 1). The galvanostatic data plotted in the right column in Figure 3 includes representative traces of up to ten cycles for each NDI. The current flowing through the cell was used to calculate the number of Lithium ions per molecule inserted into the material during the charging process (dotted lines), or the number ions released during the discharge (solid lines). On charging, the potential increases rapidly from 1 V to a value that is characteristic of each solid NDI. The potential remains at this value until either there is a new redox event, or until the material reaches the limit of its capacity at a set value of 4V. The discharge cycles (solid lines) start at 4V, rapidly reach the corresponding plateau(s), and eventually decrease to 1 V. One can appreciate from the galvanostatic cycling measurements that the relationship between aryl substitution and redox potential can be determined with more certainty from the plateau value. First reduction potential values of 2.3, 2.5, 2.6 and 2.8 V vs.  $\text{Li/Li}^+$  can be determined for compounds **7**, **6**, **8** and **9**, respectively. These values are also included in Table 1. In agreement with the cyclic voltammetry, only compound **6** (Figure 3e) displays two clear plateaus and all others display only one, despite the two-electron redox mechanism. The initial capacities achieved by compounds **6** (Figures 3e) and **9** (Figures 3h) are determined by the extent of the plateau, and approach the theoretical maximum, with the insertion of two  $\text{Li}^+$  per NDI. By comparison, compounds **7** (Figures 3f) and **8** (Figures 3g) saturate at about 0.75-1.0  $\text{Li}^+$  per NDI. Another significant feature of the galvanostatic cycling data is that the capacity for all N-hexyl compounds decreases with increasing number of cycles, likely due to the partial solubility in the electrolyte. Overall, nitrile **9** has the best initial performance (Figure

3h) with a high potential of 2.8 V vs.  $\text{Li/Li}^+$ , a single flat plateau, and an ability to reach close to 100% of its theoretical capacity ( $100 \text{ mAh g}^{-1}$ ).

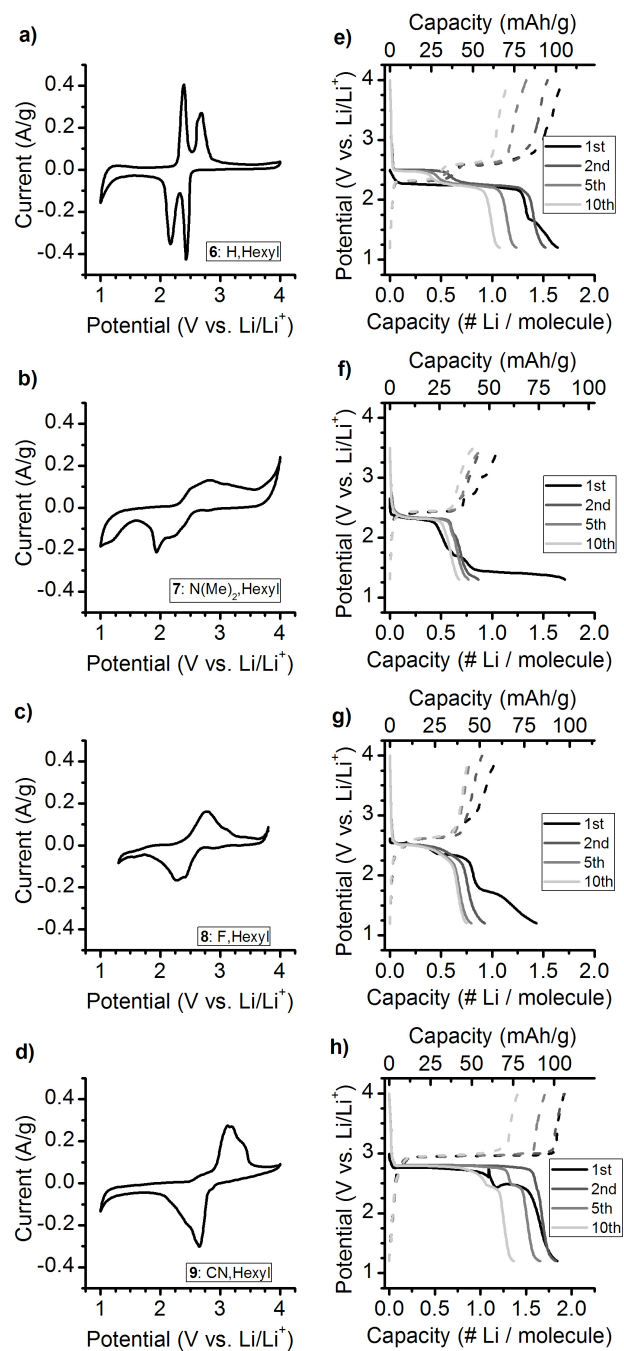
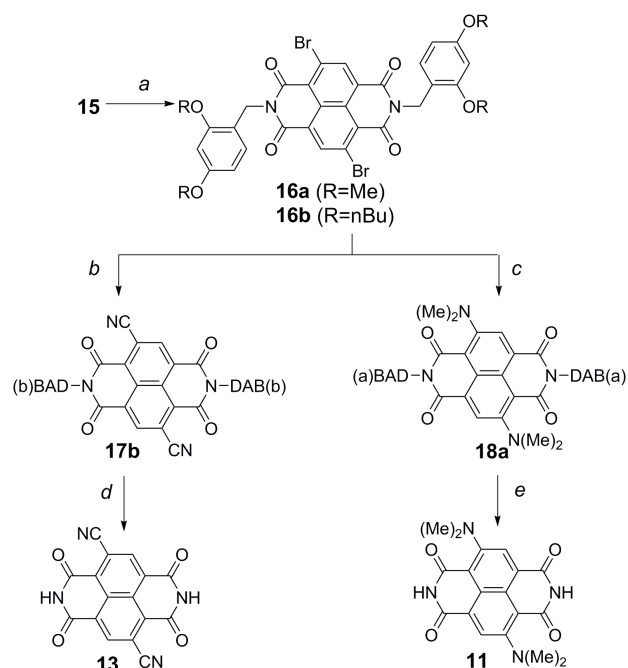


**Figure 3.** Cyclic voltammetry and cyclability of a) compound **6**, b) compound **7**, c) compound **8** and d) compound **9**. The galvanostatic cycling with electrodes prepared with e) compound **6**, f) **8** and g) **9** was carried out between 1 and 4 V vs  $\text{Li/Li}^+$ . The N,N-Dimethyl NDI **7** in f) was cycled between 1 and 3.5 V in order to avoid an irreversible oxidation above that value.

*Aryl-Substituted N-H Naphthalene Diimides.* In a separate series of experiments, we examined the question of whether the loss of capacity as a function of cycle number is determined by the solubility of the N-hexyl compounds. For this study, we

## Scheme 2



(a) Dialkoxybenzyl amine (DAB), acetic acid 120 °C; (b) CuCN, NMP 100 °C, 70%; (c) Dimethylamine, THF, 80 °C, 13% over 3 steps; (d) *i.* MeSO<sub>3</sub>H, PhMe, 110 °C; *ii.* SOCl<sub>2</sub>, DMF, 81%; (e) MeSO<sub>3</sub>H, PhMe, 110 °C, 79%.

decided to evaluate the properties of unsubstituted secondary (N-H) NDIs **10**, **11** and **13**, which are highly insoluble and nearly intractable, but can be obtained by installing a removable protecting group to assist with solubility during the synthesis and purification of all intermediates (Scheme 2). It should be noted that while one may be concerned about the acidity of this proton, previous reports show that for diimides, this proton remains uninvolved.<sup>9,10</sup> Compound **10** was prepared as reported in the literature.<sup>24</sup> The synthesis of NDIs **11** and **13** started with previously prepared dibromo substituted dianhydride **15** to prepare the 2,4-dimethoxybenzyl protected NDI **16a** by reaction with 2,4-dimethoxybenzyl amine, or the more soluble **16b**, by reaction with 2,4-di-*n*-butoxybenzyl amine (Scheme 2). The dialkoxybenzyl substituted dibromo intermediates were used to prepare the NDI **11** and **13** by S<sub>N</sub>Ar reaction with dimethylamine and Rosenmund von Braun reaction with copper cyanide followed by acid catalyzed removal of the 2,4-dialkoxybenzyl group. The use of a di-*n*-butoxybenzyl protected nitrile **17** for the synthesis of **13** was dictated by the low solubility of the dimethoxy analog, which had been suitable in the case of **18**. The required di-*n*-butoxy benzylamine was synthesized as described in the SI section (Scheme SI 1). The desired NDI **11** was obtained as a dark blue solid. It should be noted that acid catalyzed deprotection of **17** was accompanied with hydrolysis. However, the resulting solid could be easily dehydrated with thionyl chloride in dimethylformamide to yield desired NDI **13** as a grey solid.

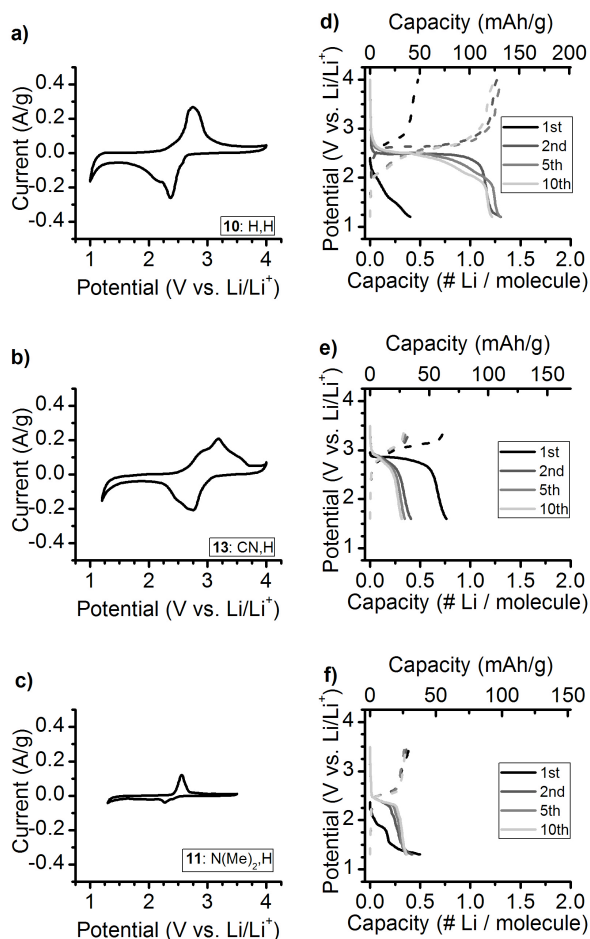


**Figure 4.** Cyclic voltammetry and galvanostatic cyclability of a) and d) compound **10**, b) and e) compound **13**, and c) and f) compound **11**.

Solid samples of compounds **10**, **11** and **13** were characterized by both cyclic voltammetry and galvanostatic cycling as shown in Figure 4. As expected, removal of the bulky N-Hexyl group reduces the solubility of the corresponding N-H compound making their handling difficult. The cyclic voltammograms are closely related to those of their N-hexyl counterparts, although compound **11** (Figure 4c) showed only minimal redox activity. A single very broad redox wave was observed for compounds **10** (Figure 4a) and **13** (Figure 4b). Although the theoretical capacity of compounds **10**, **11** and **13** increases in comparison to the N-hexyl series due to their lower molecular weight, the values obtained from the galvanostatic cycling experiments revealed significantly lower Li<sup>+</sup> insertion, with first cycle values of ~1.0 Li<sup>+</sup> for **10** (Figure 4a), 0.75 Li<sup>+</sup> for **13** (Figure e) and <0.5 for **11** (figure 4f). Despite the significantly lower solubility of all three NDIs, only the unsubstituted derivative **10** showed better capacity retention during cycling. In general, the N-H compounds have a lower utilization than the N-Hexyl analogs, suggesting that the N-H compounds may have tighter packing arrangements that prevent the intercalation of the Li<sup>+</sup> ions. Another possible explanation is that the N-Hexyl compounds may be cycling in solution rather than in the solid state, but this

is confounded by the poor capacity fade of the N-Hexyl compounds and the superior cyclability of the highly insoluble NDI **10**. Figure 5 highlights the cyclability of the three best performing NDIs. The two relatively soluble N-hexyl NDIs **9** (CN) and **6** (H) have the highest initial utilization, but their capacity decreases by ~30% over 20 cycles. In contrast, the unsubstituted NDI **10** begins with a lower utilization value but is able to maintain ~90% after 20 cycles. While it is possible that conformational degrees of freedom provided by the hexyl chains may help their crystal tolerate the structural changes required for the NDI reduction and initial insertion of the lithium ions, one could also conclude that the higher solubility compromises the integrity of the solid electrodes. Moreover, the much stronger lattice energies of the un-substituted NDI **10** appear to reduce the loss of material but also limit the amount of lithium that can be inserted in the crystal lattice.

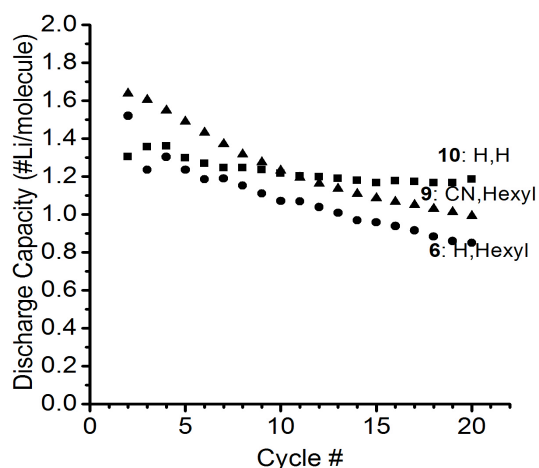


**Figure 5.** Discharge capacity vs. cycle number for three of the compounds tested. Cycling data for all compounds studied can be found in the supplementary information.

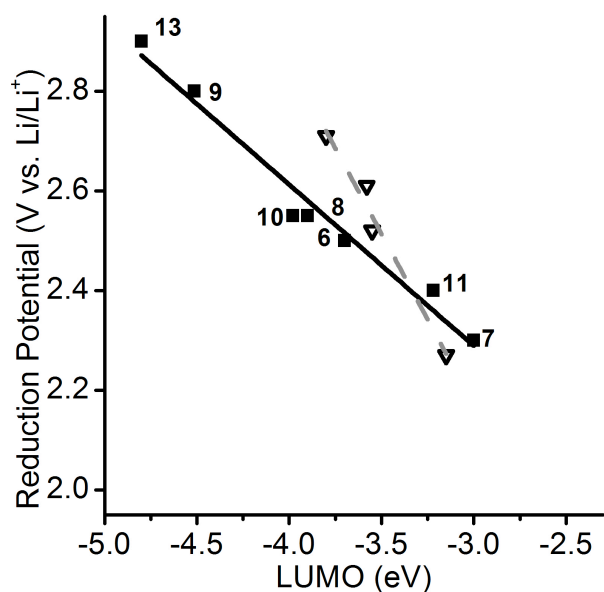


**Figure 6.** Solid state reduction potential vs. calculated gas-phase B<sub>3</sub>LYP/6-311+G(d,p) LUMO energy levels. Numbered solid squares correspond to the NDI studies here and open

triangles to heterocyclic anthraquinone analogs reported in ref. 23.

It is worth noting that the experimental reduction potentials for the organic electrodes prepared with NDIs bearing various aromatic substituents have a relatively good correlation with the gas phase electronic structure calculations computed at the B<sub>3</sub>LYP/6-311+G(d,p) level of theory. This can be readily appreciated in the calculated LUMO vs. the solid state reduction potential shown in Figure 6, which shows a linear trend. A similar correlation was recently reported by Liang *et al.*,<sup>16</sup> in a study of heterocyclic anthraquinone analogues, which also displayed a linear correlation but with a somewhat steeper slope. While two data sets are clearly too limited to draw conclusions, these results suggest that structural factors within a given compound family may dictate the relationship between the reduction potential in the gas and that in the solid state.

## CONCLUSIONS

With a starting potential of 2.55 V vs Li/Li<sup>+</sup> and 60% theoretical capacity at C/5 rate, parent naphthalene diimide **10** is both an intriguing material for lithium-ion energy storage and an excellent model system for studying the tailorability of organic electrode materials. The use of N- and aryl-substitution detailed in this article illustrates ways to control cycling performance and redox potential by influencing the solubility and electronic properties of the corresponding materials. The N-hexyl-nitrile-substituted NDI **9** has the highest utilization (90%) and second highest potential (2.8 V vs. Li/Li<sup>+</sup>) of the compounds studied. This material maintains an appreciable capacity (100 mAh/g) despite a relatively high molecular weight. Furthermore, aryl substitution with CN-, F-, and Me<sub>2</sub>N- groups allows the redox potential of the NDIs to be tailored between 2.9 and 2.3 V vs Li/Li<sup>+</sup> without significantly affecting the solubility or molecular weight. This could be a distinct advantage over standard transition-metal based lithium-ion electrode materials, whose potentials are largely confined to the energy levels of the valence states of the metal. We expect the interest in organic electrode materials such as NDI to increase as their tailorability gains greater recognition.

## AUTHOR INFORMATION

### Corresponding Author.

\*Email: Bdunn@ucla.edu, mgg@chem.ucla.edu

## ASSOCIATED CONTENT

**Supporting Information.** Synthetic details as well as characterization information (<sup>1</sup>H, <sup>13</sup>C and <sup>19</sup>F NMR, IR, and Mass Spectroscopy) can be found in associated Supporting Information. This material is available free of charge via the Internet at <http://pubs.acs.org>.

## ACKNOWLEDGMENT

We thank Y. Cao and H. Pham for computational assistance as well as E. Pierre and J. Fang for early electrochemical measurements. This work was supported by NSF IGERT: Materials Creation Training Program (MCTP) – DEG-0654431 and by grant NSF CHE-1266405 and by the Office of Naval Research (R.M. and B.D.). This material is based upon work supported by the National Science Foundation under equipment grant no. CHE-1048804.

## REFERENCES

- 1 Manthiram, A. *J. Phys. Chem. Lett.*, **2011**, 2, 176.
- 2 Goodenough, J.B.; Kim, Y. *J. Power Sources*, **2011**, 196, 6688.
- 3 Poizot, P.; Dolhem, F. *Energy Environ. Sci.*, **2011**, 4, 2003.
- 4 B. Dunn, H. Kamath, J. M. Tarascon, *Science* **2011**, 334, 928.
- 5 Alt, H.; Binder, H.; Köhling, A.; Sandsteede, G. *Electrochim. Acta.*, **1972**, 17, 873.
- 6 Chen, H.; Armand, M.; Demailly, G.; Dolhem, F.; Poizot, P.; Tarascon, J. M. *ChemSusChem*, **2008**, 1, 348.
- 7 Liang, Y.; Tao, Z.; Chen, J. *Adv. Energy Mater.*, **2012**, 2, 742.
- 8 Walker, W.; Grudgeon, S.; Vezin, H.; Laruelle, S.; Armand, M.; Wudl, F.; Tarascon, J. M. *J. Mater. Chem.*, **2011**, 21, 1615.
- 9 Renault, S.; Geng, J.; Dolhem, F.; Poizot, P. *Chem. Commun.*, **2011**, 47, 2414.
- 10 Kim, D. J.; Je, S. H.; Sampath, S.; Choi, J. W.; Coskun, A. *RSC Adv.*, **2012**, 2, 7968.
- 11 Walker, W.; Grugeon, S.; Mentre, O.; Laruelle, S.; Tarascon, J. M.; Wudl, F. *J. Am. Chem. Soc.*, **2010**, 132, 6517.
- 12 Song, Z.; Zhou, H. *Energy, Environ. Sci.*, **2013**, 6, 2280.
- 13 Nakahara, K.; Iwasa, S.; Satoh, M.; Morioka, Y.; Iriyama, J.; Suguro, M.; Hasegawa, E. *Chem. Phys. Lett.*, **2002**, 359, 351.
- 14 Sarukawa, T.; Yamaguchi, S.; Oyama, N. *J. Electrochem. Soc.*, **2010**, 12, 196.
- 15 Inamasu, T.; Yoshitoku, D.; Sumi-otorii, Y.; Tani, H.; Ono, N. *J. Electrochem. Soc.*, **2003**, 150, A128.
- 16 Liang, Y.; Zhang, P.; Yang, S.; Tao, Z.; Chen, J. *Adv. Energy Mater.*, **2013**, 3, 600.
- 17 Song, Z.; Zhan, H.; Zhou, Y. *Chem. Comm.*, **2009**, 448.
- 18 Armand, M.; Grudgeon, S.; Vezin, H.; Laruelle, S. Ribiére, P.; Poizot, P.; Tarascon, J.M. *Nature Mat.*, **2009**, 8, 120.
- 19 Song, Z.; Zhan, H.; Zhou, Y. *Angew. Chem. Int. Ed.*, **2010**, 49, 8444.
- 20 Only the N-Hexyl compounds were tested in solution, due to the lack of solubility of the X=H compounds in dichloromethane.
- 21 Würthner, F.; Osswald, P.; Schmidt, R.; Kaiser, T.; Mansikkamaki, H.; Konemann, M. *Org. Lett.*, **2006**, 8, 3765.
- 22 Dawson, R.; Hennig, A.; Weimann, D.; Emery, D.; Ravikumar, V.; Montenegro, J.; Takeuchi, T.; Gabutti, S.; Mayor, M.; Mareda, J.; Schalley, C.; Matile, S. *Nature Chem.*, **2010**, 2, 533.
- 23 Röger, C. and Würthner, F. *J. Org. Chem.*, **2007**, 72, 8070.
- 24 Sotiriou-Leventis, C.; Mao, Z. *J. Heterocyclic Chem.*, **2000**, 37, 1665.